Role of Plain Concrete in Fracture Response of Steel Fibre Reinforced Concrete Specimens

I. Havlíková [1], P. Frantík [1], H. Šimonová [1,*], V. Veselý [1], A. Abdulrahman [1], P. Schmid [2], Z. Keršner [1]

[1] *Brno University of Technology, Faculty of Civil Engineering, Institute of Structural Mechanics, Veveří 331/95, 602 00 Brno, Czech Republic*

[2] *Ditto, Institute of Building Testing*

* *simonova.h@fce.vutbr.cz*

Abstract: Load vs. crack opening displacement diagrams of fracture tests on steel fibre reinforced concrete notched specimens in a three-point bending configuration are evaluated in detail and selected results are introduced in the paper. The values of fracture parameters are determined using work of fracture method and double-K fracture model. Primarily, the role of plain concrete as a matrix in steel fibre reinforced concrete specimens is studied with regard to the recorded fracture response.

Keywords: Crack Propagation; Concrete; Steel Fibres; Three-Point Bending Test; Work of Fracture; Double-K Fracture Model.

1 Introduction

Cement-based composites are commonly used building materials. The basic representative of this type of material is concrete, a quasi-brittle composite whose range of applications can be extended using various additives, e.g. steel fibres. Even relatively small volume quantities of these fibres in concrete mixture can affect the resistance of the composite to cracking. The knowledge of mechanical fracture parameters of these materials is essential for quantification of a load-bearing capacity of cement-based composites structures and their resistance against crack initiation and propagation (i.e. the brittleness and toughness of structural members) as well as for the definition of material models used to simulate the quasi-brittle behaviour of the mentioned structures or their parts. The variability of fracture-mechanical results experimentally obtained from tests on steel fibre reinforced concrete specimens is much higher in comparison with standard concrete due to the natural heterogeneity of composite containing fibres. The main objective of this paper is to quantify the contribution of the plain concrete matrix of the steel fibre reinforced concrete specimens on their fracture response.

2 Experimental Details

The paper presents data from a wider experimental program; the focus here is on the part concerning testing of the C50/60 strength class concrete reinforced with steel fibres. For details about composition of the concrete mixture see [1]. The mixture is being developed for production of prefabricated pre-stressed concrete elements. The type of used steel fibres is Dramix 5D; the length of the fibres is 60 mm and the diameter is 0.9 mm. The dosage of fibres is 25 kg per cubic meter of fresh concrete mixture. The experiments were carried out 28 days after mixing and moulding, seven specimens from the same batch of fresh concrete were tested.

Three-point bending (3-PB) tests on notched beam specimens of nominal dimensions $150 \times 150 \times 550$ mm were conducted. The loading span was equal to 500 mm. The notch depth was about 1/3 of the specimen width; the notch was prepared by diamond saw before the test. Experiments were carried out on a Heckert FPZ 100/1 electro-mechanical testing machine. Load vs. crack mouth opening displacement (*P–CMOD*) diagrams were recorded using extensometer (crack opening displacement transducer) connected in HBM SPIDER 8 device during the fracture experiments. Informative values of compressive cube strength were determined on remaining parts of the beam specimens after 3-PB tests. For complete results of these measurements see [1].

3 Decomposition of Load vs. Crack Opening Displacement Diagrams

The measured *P–CMOD* diagrams from 7 selected 3-PB tests were used in this study. Each diagram was processed in order to obtain the component that corresponds to the structural response of the matrix of the composite consisting from plain concrete and that consisting of steel fibres reinforcing that matrix. Particular steps of the decomposition procedure for a selected specimen (III_I_28d_1) are presented in Fig. 1: first the measured *P–CMOD* diagram of the steel fibre reinforced concrete specimen is introduced; then the last part of this diagram (after the substantial drop on the curve) is predicated to be the result of contribution of steel fibres only and no effect of the concrete matrix is expected here; that part is used for a straightforward linear regression analysis to obtain an approximation of also the initial part of the diagram (polynomial function is used here with extrapolation to the origin of the *P–CMOD* space); finally a subtraction of the recorded diagram and this approximation is performed which results in the simulated *P–CMOD* diagram corresponding to the plain concrete matrix for next evaluation. Note here that the detailed analysis of the concrete matrix contribution is of particular interest within the research in this moment. Simulated diagrams corresponding to the plain concrete matrix for all remaining specimens are presented in Fig. 2.

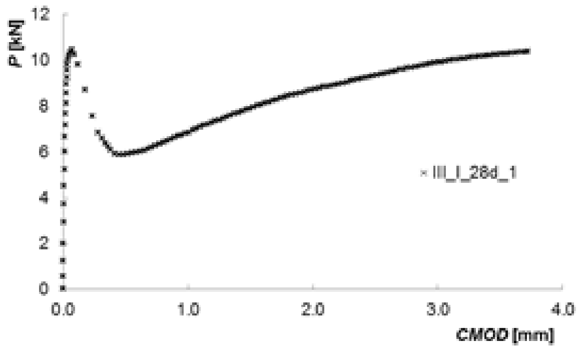

(a) measured *P–CMOD* diagram of a selected specimen

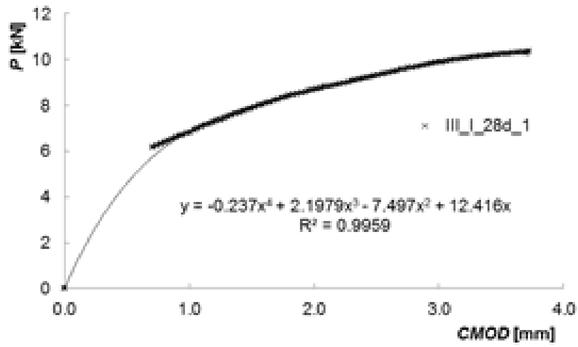

(b) procedure for estimation of the steel fibres contribution

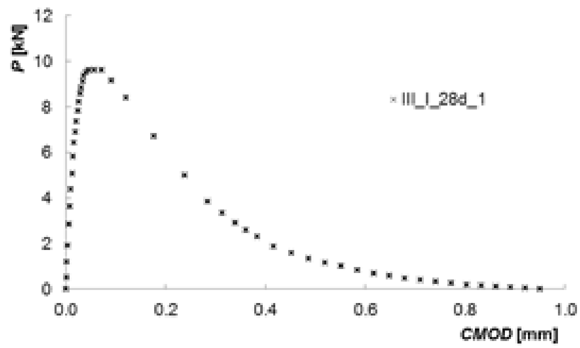

(c) simulated diagram corresponding to the plain concrete matrix

Fig. 1: Particular steps of the decomposition procedure for a selected specimen (III_I_28d_1).

4 Double-K Fracture Model and Work-Of-Fracture Method

The double-K fracture model was utilized to evaluate mechanical fracture parameters from *P–CMOD* diagrams. In principle, this model combines the concept of cohesive forces acting on the faces of the fictitious (effective) crack increment with a criterion based on the stress intensity factor – see e.g. [2]. The advantage of this model consists in a description of different levels of crack propagation: an initiation part which corresponds to the beginning of the stable crack growth (at the level where the stress intensity factor, K_{Ic}^{ini}, is reached), and a part featuring the unstable crack propagation (after the unstable fracture toughness, K_{Ic}^{un}, has been reached).

In this case, the unstable fracture toughness K_{Ic}^{un} was numerically determined first, followed by the cohesive fracture toughness K_{Ic}^{c}. When both of these values were known, the following formula was used to calculate

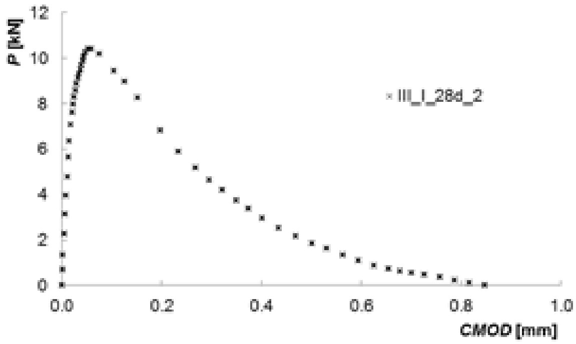

(a) *P–CMOD* diagram – specimen III_I_28d_2

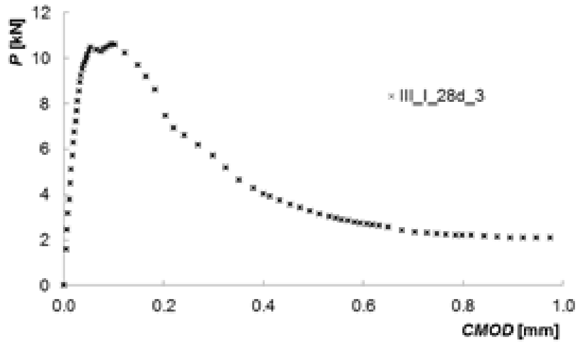

(b) *P–CMOD* diagram – specimen III_I_28d_3

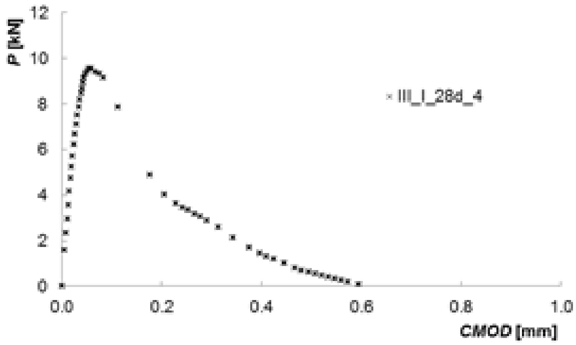

(c) *P–CMOD* diagram – specimen III_I_28d_4

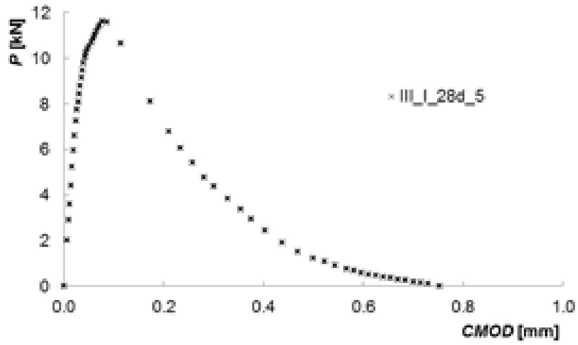

(d) *P–CMOD* diagram – specimen III_I_28d_5

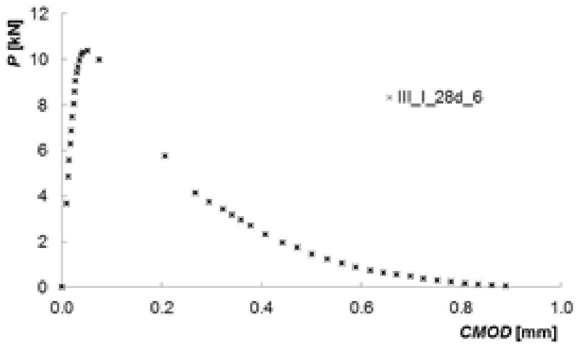

(e) *P–CMOD* diagram – specimen III_I_28d_6

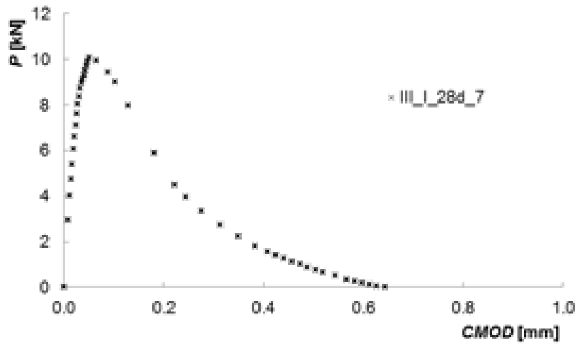

(f) *P–CMOD* diagram – specimen III_I_28d_7

Fig. 2: Simulated diagrams corresponding to the plain concrete matrix for specimens III_I_28d_2–7.

the initiation fracture toughness K_{Ic}^{ini}:

$$K_{\mathrm{Ic}}^{ini} = K_{\mathrm{Ic}}^{un} - K_{\mathrm{Ic}}^{c}. \tag{1}$$

Details regarding the calculation of both the unstable and the cohesive fracture toughness can be found e.g. in [3].

To determine the cohesive part of fracture toughness, K_{Ic}^{c}, it is necessary to accept the assumption of the distribution of the cohesive stress σ along the fictitious crack. Generally, in the cohesive crack model, the relation between the cohesive stress σ and the effective crack opening displacement, w is referred to as the cohesive stress function $\sigma(w)$. The cohesive stress σ (*CTOD$_c$*) at the tip of the initial notch of length a_0 at the critical state can be obtained from the softening curve. In this paper, the bilinear softening curve was used when two cases may occur:

In case I ($CTOD_c \leq w_s$), σ ($CTOD_c$) value can be obtained according to:

$$\sigma\left(CTOD_c\right) = f_t - \left(f_t - \sigma_s\right)\frac{CTOD_c}{w_s}, \tag{2}$$

where f_t is the tensile strength, $CTOD_c$ is critical crack tip opening displacement (see e.g. [2]), σ_s and w_s

are the ordinate and abscissa at the point of slope change of the bilinear softening curve, respectively. According to Petersson [4], the σ_s and w_s values can be considered using the following equations:

$$\sigma_s = \frac{1}{3} f_t \text{ and } w_s = \frac{2}{9} w_c, \tag{3}$$

where w_c is the critical crack tip opening displacement. In this paper, w_c is constant value (w_c = 0.16 mm) for all specimens.

The value of tensile strength is estimated using the measured value of compressive strength f_{cu} using the following relation [5]:

$$f_t = 0.24 f_{cu}{}^{\frac{2}{3}}. \tag{4}$$

In case II ($w_s \leq CTOD_c \leq w_c$), $\sigma(CTOD_c)$ value can be calculated using the following formula:

$$\sigma\left(CTOD_c\right) = \frac{\sigma_s}{w_c - w_s}\left(w_c - CTOD_c\right). \tag{5}$$

Fracture energy G_{F} is defined as the energy needed to create a crack surface of unit area. Similarly to the "work-of-fracture method" [6], the fracture energy G^*_{F} used in this study is calculated as the area under the *P–CMOD* curve recorded during the fracture test and divided by the area of the initial specimen ligament. The authors are aware that the work of external forces is calculated as the multiplication of the load P and the displacement d at the load-point application, which was not recorded here (but the *CMOD* was). Therefore, it is not possible to determine the precise value of G_{F} from the *P–CMOD* curve. Thus, its affine value G^*_{F} is studied here.

To approach the value of the part of "true fracture energy" two limit values of that quantity as the estimations for its lower and upper bounds were determined for selected stages of the fracture process. Lower (upper) limit value for each step was set up according to Eq. (6). In each case a section of the area under the *P–CMOD* curve (estimated by two the different ways) was employed for the calculation of the corresponding part of the work of fracture value. The mentioned ways of the work of fracture estimations are shown at Fig. 3 for both the upper as well as the lower limit value. To obtain the corresponding value of specific fracture energy the appropriate work of fracture value is divided by the area which corresponds to current effective crack increment (Fig. 3). This approach can be applied with respect to actual value of *CMOD*$_i$. Bunch of described G^*_{F} values for *CMOD*$_i$ between 0 and 1 mm (at *CMOD* values ā 0.2 mm) can be found in Fig. 4.

$$G^*_{\mathrm{F,min}} = \frac{W^*_{\mathrm{F,min}}}{B\left(a_{\mathrm{e}} - a_0\right)}, \qquad G^*_{\mathrm{F,max}} = \frac{W^*_{\mathrm{F,max}}}{B\left(a_{\mathrm{e}} - a_0\right)} \tag{6}$$

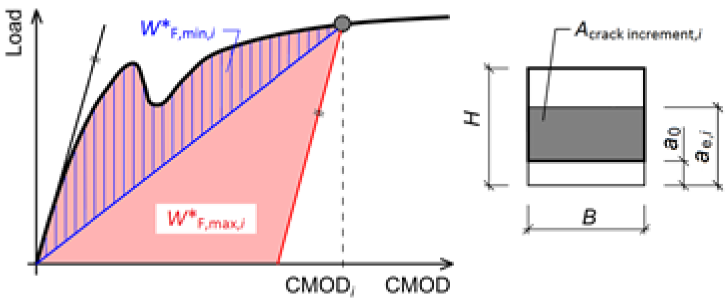

Fig. 3: To evaluation of minimal and maximal part of fracture energies corresponding to *CMOD*$_i$ [1].

It should be noted here, that definition of the $G^*_{\mathrm{F,max}}$ is somehow controversial. The parallel trend of the initial and the unloading line actually indicates that no crack has been propagated up to this stage of the loading process because no increase in the specimen compliance is observed. Thus, the $G^*_{\mathrm{F,max}}$ value shall tend to infinity as the crack increment $a_e - a_0$ converges to zero. In reality, the diversion of the unloading compliance of the specimen indicates some level of "plastic" behaviour which means that a certain amount of energy is dissipated in a propagating nonlinear zone. Estimation of the nonlinear zone extent (and its other parameters, like the energy dissipation density) is tricky task and is out of scope of this study. Therefore, a distinct inaccuracy is adopted in the analysis evaluating the $G^*_{\mathrm{F,max}}$ value. This quantity should be taken into account as an informative parameter.

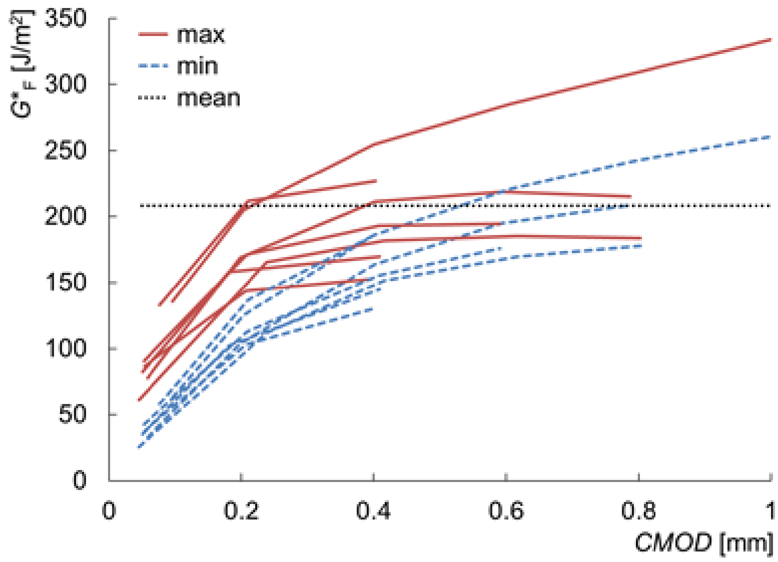

Fig. 4: Bunch of values of parts of minimal and maximal specific fracture energy $G^*_{\mathrm{F,min}}$ and $G^*_{\mathrm{F,max}}$ with respect to actual *CMOD* for the plain concrete matrix of the steel fibre reinforced composite; mean value of $G_{\mathrm{F}}{}^*$ is also depicted.

Tab. 1: Mean values of selected parameters (coefficients of variation in %) and their relative values with respect to the plain concrete matrix of steel fibre reinforced concrete (1.00 [–]).

	Plain concrete (matrix of SFRC)	Steel fibre reinforced concrete (SFRC)
f_{cu} [MPa]	- | -	86.3 (2.3) | -
f_t [MPa]	- | -	4.68 (1.5) | -
E [GPa]	30.2 (21.3) | 1.00	25.5 (12.0) | 0.84
K^{un}_{Ic} [MPa.m$^{1/2}$]	1.471 (17.6) | 1.00	1.715 (18.5) | 1.17
$K^{ini}_{\mathrm{Ic}}/K^{un}_{\mathrm{Ic}}$ [-]	0.190 (29.3) | 1.00	0.330 (12.4) | 1.74
G^*_{F} [J/m^2]	208.22 (1.5) | 1.00	3606.3 (23.5) | 17.31

5 Results

Mean values (and coefficients of variation) of selected results are summarized in Tab. 1: compressive strength f_{cu}, tensile strength f_t (estimated according to Eq. (4), elasticity modulus E, fracture toughness K^{un}_{Ic}, the $K^{ini}_{\mathrm{Ic}}/K^{un}_{\mathrm{Ic}}$ ratio, i.e. the ratio expressing the (load level/crack length) difference between the stable and onset of the unstable crack propagation, and specific fracture energy obtained using *P–CMOD* diagram G^*_{F}, respectively. In this table the relative values of these parameters are also introduced – 1.00 corresponds to the mean value of the selected parameters for plain concrete matrix of steel fibre reinforced concrete.

6 Conclusion

The role of plain concrete matrix of steel fibre reinforced concrete specimens at the age of 28 days in their fracture response was quantified using decomposition of the measured load vs. crack opening displacement diagrams. It follows from the analysis that fibres affected values of all the studied mechanical fracture parameters: slight decrease in elasticity modulus (about 16 %), slight increase in fracture toughness (17 %), substantial increase in difference between the stable and onset of the unstable crack propagation (74 %), and of course diametrical increase in informative specific fracture energy (more than 17×) is observed. It can be concluded this procedure generates outputs usable for adequate evaluation of the effect of fibres to the fracture behaviour of the resulting composites.

Acknowledgement

Support from the Czech Scientific Agency (project No. P104-13-03662S) and the Ministry of Education, Youth and Sports of the Czech Republic under the “National Sustainability Programme I” (project No. LO1408) is gratefully acknowledged.

References

[1] D. Lehký et al., Advanced Evaluation of Fracture Response of Steel Fibre Reinforced Concrete Specimens: submitted to Special ASCE CONCREEP conference proceeding (2015), Vienna.

[2] S. Kumar, S. V. Barai, Concrete Fracture Models and Applications, Springer, Berlin, 2011.

[3] X. Zhang, S. Xu, A comparative study on five approaches to evaluate double-K fracture toughness parameters of concrete and size effect analysis, Engineering Fracture Mechanics 78 (2011) 2115–2138.

[4] P. E. Petersson, Crack growth and development of fracture zone in plain concrete and similar materials, Report No. TVBM-1006, Lund Institute of Technology, 1981.

[5] V. Červenka, L. Jendele, J. Červenka, ATENA Program documentation – Part 1: theory. Červenka Consulting, Praha, 2012.

[6] RILEM Committee FMT 50, Determination of the fracture energy of mortar and concrete by means of three-point bend test on notched beams, Materials & Structures 18 (1985) 285–290.